Microalloying Additions and HAZ Fracture Toughness in HSLA Steels

An extensive study evaluates the effects of Ti, V and Nb on CTOD toughness at various heat inputs

BY G. R. WANG, T. H. NORTH AND K. G. LEEWIS

ABSTRACT. The HAZ fracture toughness properties of HSLA steels containing controlled combinations of microalloying elements (Ti, V, Nb) are evaluated at heat inputs ranging from 3 to 6 kJ/mm (76 to 152 kJ/in.).

Steel microalloyed with a combination of titanium, niobium and vanadium had much poorer toughness properties than steel alloyed with titanium alone. Increasing silicon content in steel alloyed with titanium had a detrimental effect only on fracture toughness properties in welds made at a heat input of 3 kJ/mm. At 6 kJ/mm heat input, this detrimental influence of higher silicon content was not apparent. In the case of lower carbon content in steel alloyed with titanium only, the fracture toughness values were marginally poorer when welding at high heat input (6 kJ/mm).

Increasing heat input from 3 to 6 kJ/mm improved the HAZ fracture toughness properties of steel containing 0.093% V, and had a particularly detrimental effect on the toughness of steel alloyed with vanadium and titanium in high heat input welding situations.

Introduction

The heat-affected zone (HAZ) fracture toughness properties of HSLA steels remain the key when determining the structural integrity of major installations. Although HAZ toughness has received considerable attention (Ref. 1), there is a need for a systematic study of the influence of different combinations of microalloying elements (Nb, V, Ti) on HAZ fracture toughness properties. In particular, the study used laboratory-made steels of closely controlled chemistry, welded at a range of heat input levels.

G. R. WANG is a Visiting Scientist and T. H. NORTH is a Professor at the University of Toronto, Toronto, Ont., Canada. K. G. LEEWIS is also a Professor at the University of Toronto, Toronto, Ont., Canada.

The Welding Institute of Canada has been carrying out an extensive research program evaluating the fracture toughness properties of HAZ regions in constructional steels. This paper presents some of the results from this extensive study.

Background

The heat-affected zone toughness properties in HSLA steels depend on the complex interplay of microstructure, grain size, particle (carbonitride, nitride) dissolution and reprecipitation, and plate chemistry. It is well known that niobium and vanadium carbonitrides dissolve during the heating cycle of fusion welding, and reprecipitate if the cooling rate is slow enough (Refs. 1–3). It follows that the effect of any microalloying addition (such as niobium) on HAZ toughness properties depends markedly on the heat input used (on the thermal cycle enabling particle solution, possible reprecipitation and subsequent hardening), and on the effect of soluble niobium on the phase transformations occurring during cooling after welding. In HSLA steels alloyed with niobium only, the cooling time is the dominant factor (Ref. 4). At short cooling times (6.5 to 16 s for the 800°/500°C – 1472°/932°F temperature range) niobium has a beneficial influence on HAZ toughness. Yet, in higher heat input (slower cooling rate) welding situations, niobium has a detrimental effect on toughness values.

KEY WORDS

Microalloying
HSLA steels
Fracture Toughness
HAZ Toughness
Ti/V/Nb Effects
Ti Toughness Effect
Ti Effect/HSLA Steel
Detrimental Effects
Constructional Steel
Poor HAZ Toughness

The situation is more complicated when different combinations of microalloying elements are present in the steel. The effect of titanium, titanium plus niobium, and titanium plus vanadium additions on the HAZ toughness properties of linepipe steel were evaluated by McCutcheon (Ref. 5). When welding at 2 kJ/mm heat input, niobium additions to titanium-bearing steel decreased toughness values as a result of significant solute strengthening. Vanadium in combination with titanium improved HAZ toughness values, and vanadium additions to a 0.05%-niobium-bearing steel produced a slight fall-off in toughness properties. Precipitate dissolution and reprecipitation during the weld thermal cycle are also affected when different combinations of microalloying elements are present. Suzuki and Weatherly (Ref. 3) observed that in steels containing titanium plus niobium, niobium-rich precipitates dissolved and titanium-rich particles reprecipitated later in the heating cycle. This reprecipitation effect explained the finer HAZ grain sizes in Ti-Nb-containing steels.

Yamamato (Ref. 6) has suggested that the effect of any microalloying addition on HAZ toughness depends markedly on the type of precipitate present in the base material prior to welding. In base material containing a dispersion of TiN precipitates, higher niobium contents were detrimental since niobium microsegregation around TiN particles enhanced hardenability and suppressed acicular ferrite nucleation. On the other hand, in base material containing a dispersion of Ti_2O_3 particles, increasing niobium content had no effect on HAZ toughness values.

Lau, Wang and North (Ref. 7) have recently examined the HAZ fracture toughness of HSLA steels containing different combinations of niobium, vanadium and titanium. When welding at 3 and 6 kJ/mm heat input, the poorest fracture toughness properties were produced in steel alloyed with niobium, vanadium and titanium.

Table 1—Steel Compositions

Code	C	Mn	Si	V	Nb	Ti	Al	N	P	S	O
50	0.11	1.33	0.26	0.082	0.027	0.016	0.058	0.010	0.004	0.005	0.0057
51	0.12	1.36	0.28	0.080	<0.005	0.014	0.049	0.008	0.003	0.005	0.0060
52	0.11	1.35	0.27	<0.003	0.026	0.015	0.054	0.009	0.004	0.005	0.0067
53	0.11	1.35	0.26	<0.003	<0.005	0.014	0.055	0.009	0.004	0.005	0.0057
55	0.11	1.34	0.56	<0.003	<0.005	0.014	0.049	0.009	0.004	0.006	–
56	0.077	1.44	0.56	<0.003	<0.005	0.015	0.050	0.009	0.004	0.006	–
58	0.13	1.41	0.29	0.093	<0.005	<0.002	0.053	0.008	0.004	0.004	0.0068
59	0.13	1.52	0.29	<0.003	0.029	<0.002	0.052	0.009	0.004	0.004	0.0065

Steel microalloyed with titanium only produced the highest HAZ fracture toughness properties at both heat input levels. This paper presents further results from the detailed study, *viz.*, evaluating:

1) The effect of microalloy content on the 0.1 mm CTOD transition temperature for welds deposited at 3, 4, 5 and 6 kJ/mm heat input.

2) The effect of increasing silicon content, and decreasing carbon content on the fracture toughness of steel alloyed with titanium only. Since the HSLA steel alloyed with titanium only produced the highest HAZ toughness properties (Ref. 7), it was particularly important to evaluate the influence of changes in silicon and carbon on the performance of this material.

Experimental Procedure

Materials

All steels were laboratory-made, with discrete changes in microalloying element concentrations as the principal variables in fracture toughness testing. The Mn content of all steels was similar to that of Canadian controlled-rolled steels. No boron, calcium or molybdenum additions were made to the laboratory-made chemistries. The plate compositions involved were Steel 50 (Nb, V, Ti), Steel 51 (V, Ti), Steel 52 (Nb, Ti), Steel 53 (Ti only), Steel 58 (V) and Steel 59 (Nb).

The effect of increasing silicon content (Steel 55) and decreasing carbon content (Steel 56) on the fracture toughness of titanium-bearing steel was also evaluated—Table 1.

The plate production procedure comprised laboratory melting of 150 kg (330 lb) ingots, reheating at 1150°C (2102°F) and hot rolling to make 375 × 150 × 25-mm (15 × 6 × 1-in.) thick specimens. This specimen-manufacturing procedure was maintained constant for all the steels tested in this study.

Welding Conditions

Linde 40 welding wire and Oerlikon OP121TT flux were used during all submerged arc welding tests.

Welds were deposited at 3, 4, 5 and 6 kJ/mm (76, 102, 127 and 152 kJ/in.) heat input. Table 2 shows the welding parameters employed. For these heat input levels, the cooling times between 800° and 500°C were 16.9 s (3 kJ/mm), 28.9 s (4 kJ/mm), 42.4 s (5 kJ/mm) and 55.6 s (6 kJ/mm), respectively.

Fracture Toughness Testing

All fracture testing was carried out using the CTOD test, since CTOD and Charpy toughness/temperature transition relations do not necessarily correspond for any given steel composition. Also, there is a move to include HAZ CTOD toughness values in many specifications, so the CTOD approach was used in this work. All HAZ fracture toughness testing was carried out using t × t, 10 × 10 × 50-mm (0.4 × 0.4 × 2.0-in.) CTOD specimens, oriented transverse to the welding direction—Fig. 1.

Each CTOD specimen was subjected to careful preparation to ensure that the fatigue crack tip was located in the coarse-grained HAZ. After the specimen width, B, was obtained by grinding, both surfaces were polished and etched to determine the fusion boundary position. The specimen depth was then marked on the polished surface so that the fusion boundary was just beyond the mid-depth, W/2, and machining was then completed. This put the notch tip and coarse-grained HAZ exactly at mid-depth, W/2; the resultant a/W values were approximately 0.5.

The fatigue crack normally exhibits a curved front with the depth at midpoint being greater than at the edge of the specimen. In CTOD testing, initiation usually occurs at some point near the center of the specimen. This means that the fatigue crack growth measured on the surface must be corrected so that the crack tip is located exactly within the coarse-grained zone. The assumption of using a fixed difference between surface and actual crack depth was verified by sectioning CTOD specimens after testing (to confirm that the notch tip was properly located in the desired region).

Table 2—Summary of Welding Parameters

Nominal Heat Input kJ/mm	Voltage	Amperes	Travel Speed (mm/s)
3	32	600	6.25
4	32	650	5.00
5	34	700	4.58
6	35	750	4.17

Three to five CTOD specimens were tested at −70°, −50°, −30°, −5°C (−94°, −58°, −22, 23°F), and at room temperature. The minimum CTOD values at any temperature for any steel chemistry were taken as the indicator of fracture toughness properties in this work. No matter the scatter in test results, this approach was strictly followed. This approach necessarily means that the results show the worst-case situation.

Table 3 shows the CTOD values and the type of fracture behavior (δc, δu and δm values) produced when testing Steel 53 (Ti only), Steel 55 (effect of increasing

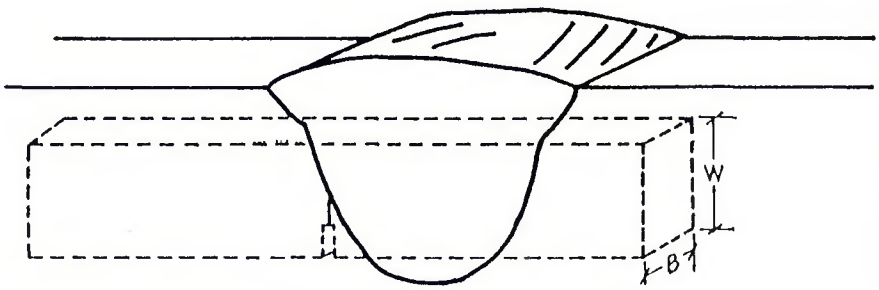

Fig. 1—Orientation of CTOD test piece with respect to weld bead, showing position of precrack.

Table 3—Minimum CTOD Fracture Toughness Values (mm) for Steels 50, 53, 55 and 56

Code	Heat Input kJ/mm	Temperature (°C) −70°	−50°	−30°	−5°	22°
Steel 53	3	0.056 (δu)[a]	0.086 (δu)	0.307 (δm)[a]	—	0.322 (δm)
(Ti)	4	0.058 (δu)	0.069 (δu)	0.307 (δu)	0.241 (δm)	0.320 (δm)
	5	0.030 (δc)[a]	0.168 (δu)	0.165 (δu)	0.356 (δu)	0.361 (δm)
	6	0.053 (δu)	0.119 (δu)	0.122 (δu)	0.358 (δu)	0.396 (δm)
Steel 55	3	0.032 (δc)	0.064 (δu)	0.091 (δu)	0.086 (δu)	0.279 (δm)
(Si, Ti)	6	0.048 (δu)	0.086 (δu)	0.134 (δu)	0.328 (δm)	0.346 (δm)
Steel 56	3	0.002 (δu)	0.114 (δu)	0.247 (δu)	0.230 (δm)	0.295 (δm)
(C, Ti)	6	0.028 (δc)	0.062 (δu)	0.141 (δu)	0.220 (δu)	0.326 (δm)
Steel 50	3	—	0.03 (δc)	0.033 (δc)	0.048 (δu)	0.124 (δm)
(Nb,V,Ti)	6	—	—	0.018 (δc)	0.028 (δc)	0.061 (δu)

(a) The type of fracture is indicated as δc, δu or δm.

Table 4—Results of Hardness Measurements of HAZ[a]

Steel	3 kJ/mm	4 kJ/mm	5 kJ/mm	6 kJ/mm
50 (Nb, V, Ti)	253 ± 9	233 ± 5	228 ± 7	221 ± 5
51 (V, Ti)	221 ± 6	215 ± 6	210 ± 5	201 ± 4
52 (Nb, Ti)	219 ± 3	214 ± 6	208 ± 4	203 ± 5
53 (Ti)	215 ± 5	209 ± 6	200 ± 3	198 ± 4
55 (Ti, Si)	207 ± 5	200 ± 4	201 ± 8	191 ± 7
56 (Ti, C)	211 ± 8	202 ± 6	199 ± 6	189 ± 7
58 (V)	234 ± 7	235 ± 7	213 ± 5	210 ± 7
59 (Nb)	224 ± 6	214 ± 5	212 ± 3	205 ± 8

(a) Vickers 1000 g load.

Si content) and Steel 56 (effect of lower-carbon steel).

Hardness and Tensile Testing

Twenty HAZ hardness values were taken on each sample. The hardness values produced at 3, 4, 5 and 6 kJ/mm are presented in Table 4. The tensile strength properties of the steels tested are presented in Table 5.

Metallography

The prior austenite grain size adjacent to the fusion line was evaluated by counting approximately 50 grains in the direction parallel to fusion boundary. In low heat input welding situations (3 and 4 kJ/mm), there was some grain elongation at right angles to the fusion line—Table 6.

During detailed examination of HAZ microstructures, the following microstructural classification was employed, *viz.*, proeutectoid or grain boundary ferrite (GF), ferrite sideplates (SP) and intragranular constituents (IC), comprising ferrite with carbide and/or martensite-austenite (M-A) constituent. The HAZ microstructures were not evaluated at the site of crack initiation along the fatigue crack front. All microstructural evaluations were taken in the HAZ region where the notch was located during CTOD testing. The metallographic specimens were cut from the same welds that were examined during fracture testing.

Point counting was carried out at 500X magnification using a binocular eyepiece with a 5 × 11 grid. Ten grids (550 points) were counted on each weld cross-section. Since two cross-sections were examined, a total of 1100 points was counted on each test weld. These data are presented in Table 7.

The (M-A) phase content was evaluated by etching and staining test samples with the Le Pera etch. This etchant stained the ferrite grey, the carbides black and the (M-A) phase remained white. These data are also presented in Table 7.

Results

Figures 2 to 4 show the 0.1 mm CTOD transition temperature/heat input relations for the steels tested. It is apparent that:

1) Steel 53 (Ti only) produced the best fracture toughness properties at all heat input levels. Steel 50 (Nb, V, Ti) produced the poorest fracture toughness values at 3 and 6 kJ/mm heat inputs.

2) Increasing heat input raised the 0.1 mm CTOD transition temperature by >30°C (54°F) in the case of Steel 51 (V, Ti) and Steel 50 (Nb, V, Ti). In the case of Steel 59 (Nb), Steel 53 (Ti) and Steel 56 (C, Ti) the 0.1 mm CTOD values were raised by approximately 15°C (27°F).

3) HAZ fracture toughness properties markedly improved in Steel 58 (V) and Steel 55 (Si, Ti) when heat input was raised from 3 to 6 kJ/mm.

The titanium-bearing steels had the finest grain sizes, the Steel 50 (Nb, V, Ti) having the smallest values. On the other hand, Steel 50 (Nb, V, Ti) also had the highest HAZ hardness values—Tables 4 and 6.

HAZ microstructures comprised proeutectoid or grain boundary ferrite, ferrite sideplates and intragranular constituents (ferrite with carbide and/or martensite (M-A) constituent). The beneficial effect of increasing heat input on the fracture toughness of vanadium-bearing steel (Steel 58) was associated with the fine acicular ferrite-like HAZ microstructure—Fig. 5. This HAZ microstructure is compared with those in Steel 53 (Ti) and Steel 50 (Nb, V, Ti) in Figs. 6 and 7.

Figures 8 to 10 compare CTOD values, HAZ grain size and hardness values in

Table 5—Tensile Strength Properties

Sample Identification	Yield Strength, MPa (ksi) Upper Longitudinal	Upper Transverse	0.2% offset Longitudinal	0.2% offset Transverse	Ultimate Tensile Strength MPa (ksi) Longitudinal	Ultimate Tensile Strength Transverse	Percent Elongation in 25 mm (1 in.) Longitudinal	Percent Elongation Transverse
50 (Nb, V, Ti)	419 (60.7)	361 (52.3)	383 (55.6)	338 (49.1)	538 (78.0)	519 (75.2)	30.5	26.5
51 (V, Ti)	381 (55.3)	353 (52.0)	340 (49.4)	324 (47.1)	492 (71.4)	483 (70.1)	36.5	31.5
52 (Nb, Ti)	468 (67.9)	392 (56.8)	360 (52.2)	343 (49.8)	490 (71.1)	478 (69.3)	38	35
53 (Ti)	351 (51.0)	345 (50.0)	314 (45.6)	310 (44.8)	472 (68.5)	470 (68.2)	40.5	35
55 (Ti, Si)	368 (53.4)	358 (51.9)	331 (48.0)	327 (47.4)	509 (73.9)	493 (71.5)	32.5	37
56 (Ti, C)	403 (58.5)	369 (53.6)	328 (47.6)	314 (45.6)	473 (68.7)	467 (67.7)	38	35.5
58 (V)	483 (70.1)	413 (60.0)	423 (61.3)	394 (57.1)	569 (82.6)	555 (80.6)	31	31
59 (Nb)	483 (70.1)	423 (61.4)	404 (58.6)	370 (53.6)	523 (75.9)	509 (73.8)	34.5	35

Table 6—Average HAZ Grain Size at Fusion Line

Steel	A	B	C	D
50 (Nb, V, Ti)	78.8 ± 20.2 (103.5 ± 31.2)[a]	103.2 ± 28.3 (109.2 ± 25.4)	124.8 ± 24.7	133.3 ± 32.8
51 (V, Ti)	88.6 ± 20.1 (96.6 ± 17.8)	116.7 ± 27.4 (123.7 ± 29.3)	138.0 ± 18.9	150.8 ± 35.1
52 (Nb, Ti)	79.6 ± 21.1 (83.0 ± 27.4)	106.0 ± 36.2 (112.0 ± 27.9)	123.1 ± 37.5	147.3 ± 38.2
53 (Ti)	87.2 ± 31.4 (95.7 ± 28.3)	101.7 ± 21.4 (110.2 ± 18.2)	135.7 ± 27	155.0 ± 32
55 (Ti, Si)	84.9 ± 29.9 (91.2 ± 27.4)	125.1 ± 23 (130.5 ± 27.1)	151.8 ± 32.8	168.0 ± 37
56 (Ti, C)	109.8 ± 14.7 (115.9 ± 16.9)	140.5 ± 15.1 (153.0 ± 19.4)	171.0 ± 48.8	193.9 ± 33.1
58 (V)	114.3 ± 34.8 (122.3 ± 41.2)	170.2 ± 60.2 (175.1 ± 59.4)	185.3 ± 45.2	203 ± 72.1
59 (Nb)	78.3 ± 14.1 (84.3 ± 17.5)	98.9 ± 9.5 (103.8 ± 11.7)	143.4 ± 23.4	199.2 ± 35

(a) Figures in parentheses are grain sizes measured perpendicular to the fusion line. All figures in μm.

Table 7—Quantitative Microstructural Analyses

Steel	Structure %	Heat Input kJ/mm 3	4	5	6	Description of Intragranular Components
53 (Ti)	%G.F.[a]	5.1	7.2	9.5	11.9	At 3 kJ/mm heat input, about 20% of the intragranular components were bainite, the remainder was a mixture of acicular ferrite and pearlite. The bainite colony size was comparable to that of Steel 50. As heat input increased, the bainite content decreased and was replaced by acicular ferrite, which had a very large (>5:1) aspect ratio. At 6 kJ/mm heat input, only acicular ferrite was observed
	%S.F.[b]	6.0	8.7	10.5	10.7	
	%I.C.[c]	88.9	84.1	80.0	77.4	
(M-A) phase		1.6	–	–	–	
55 (Ti, Si)	%G.F.	5.3	6.5	9.6	12.5	The intragranular constituents were composed mostly of ferrite laths, with occasional bainitic patches. The ferrite laths had high aspect ratios and experienced preferential growth in particular crystallographic directions as the laths cross each other roughly at right angles. At higher heat inputs, large ferrite laths intermixed with smaller ferrite grains were apparent.
	%S.F.	6.2	6.8	8.1	4.7	
	%I.C.	88.5	86.7	81.3	82.8	
(M-A) phase		1.8	–	–	–	
56 (Ti,C)	%G.F.	5.0	8.0	8.4	10.7	There were many fine second phase particles (carbon/(M/A)) embedded in the ferrite phase, even at prior austenite grain boundaries. The intragranular constituents were composed mostly of irregularly shaped ferrite plates embedded with second phase particles. The microstructures are coarser than in other steels. At higher inputs, the intragranular ferrite plates became much coarser, although they were fewer in number.
	%S.F.	5.1	10.7	8.5	8.3	
	%I.C.	89.9	81.3	83.1	81.0	
(M-A) phase		1.0	–	–	–	
51 (V,Ti)	%G.F.	4.9	5.8	7.2	9.0	The intragranular structures consisted of a mixture of acicular ferrite, equiaxed ferrite and bainitic structures. At 3 kJ/mm there was approximately 50% bainite and the colony size was coarser than that observed in the other steels. At higher heat inputs, more coarse equiaxed ferrite was observed, replacing part of the acicular ferrite phase. The bainite colonies were coarser.
	%S.F.	5.6	8.3	11.7	9.8	
	%I.C.	90.5	85.9	81.1	81.2	
(M-A) phase		0.0	–	–	–	
52 (Nb,Ti)	%G.F.	4.5	6.1	7.8	10.1	The intragranular components and grain boundary ferrite content were similar to that in Steel 51. The sideplate ferrite content did not change markedly with increasing heat input. In comparison with Steel 51, bainite colony sizes were finer at 3 kJ/mm heat imput. No change in bainite colony size occurred at 6 kJ/mm heat input.
	%S.F.	10.0	11.4	13.5	11.3	
	%I.C.	85.5	82.5	78.7	78.6	
(M-A) phase		2.2	–	–	–	
59 (Nb)	%G.F.	1.7	2.5	3.5	4.1	Large bainite colonies were observed in low heat input welds. Although increasing heat input had no effect on bainite colony size, the substructure of these regions became coarser. More grain boundary ferrite was present in high heat input welds.
	%S.F.	2.4	3.2	4.3	4.7	
	%I.C.	95.9	94.3	92.2	91.2	
(M-A) phase		0.6	–	–	–	

(a) G.F. = grain boundary ferrite. (b) S.F. = sideplate ferrite. (c) I.C. = intragranular ferrite.

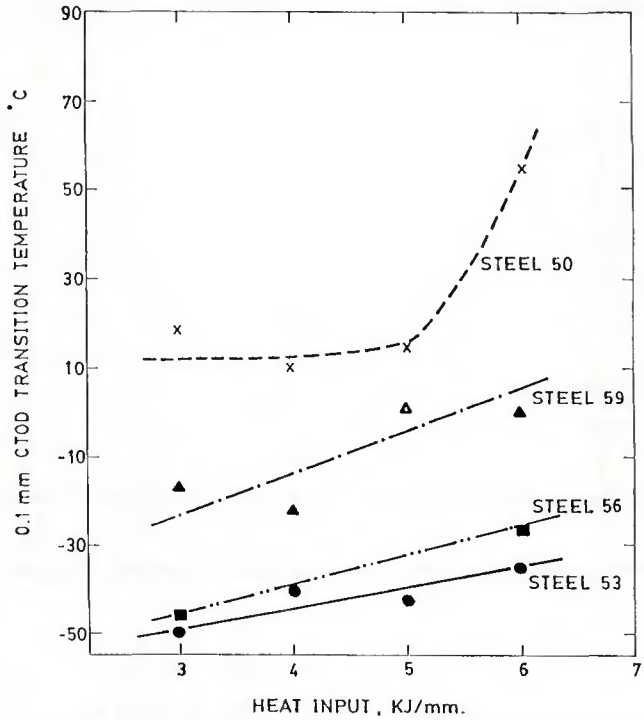

Fig. 2 – 0.1 mm CTOD transition temperature/heat input relations for Steel 50 (Nb, V, Ti), Steel 53 (Ti), Steel 56 (C, Ti) and Steel 59 (Nb).

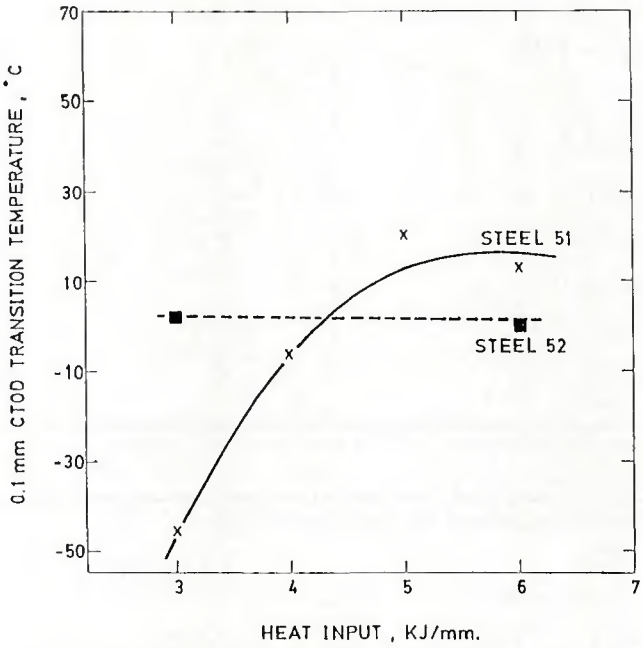

Fig. 3 – 0.1 mm CTOD transition temperature/heat input relations for Steel 51 (V, Ti) and Steel 52 (Nb, Ti).

Steels 53 (Ti) and 55 (Ti, high Si). Increasing silicon content from 0.26% (Steel 53) to 0.56% (Steel 55) had a particularly detrimental effect on the fracture toughness at 3 kJ/mm heat input. The detrimental influence of silicon on the toughness of steel alloyed with titanium only disappeared at high heat input (6 kJ/mm). Steel 55 was slightly softer than Steel 53 and HAZ grain size was greater at all heat input levels above 3 kJ/mm.

Figures 9 to 11 compare CTOD values, HAZ grain size and hardness when the carbon content was decreased in Steel 53 (Ti). Lowering the carbon from 0.11 to 0.077% in Steel 56 had a detrimental effect on the fracture toughness of 3 kJ/mm heat input weld deposits. At higher heat input (6 kJ/mm) the fracture toughness properties were also lowered when specimens were tested at temperatures above −30°C (−22°F). The HAZ in Steel 56 was softer than in Steel 53, and the HAZ grain size was larger at all heat input levels.

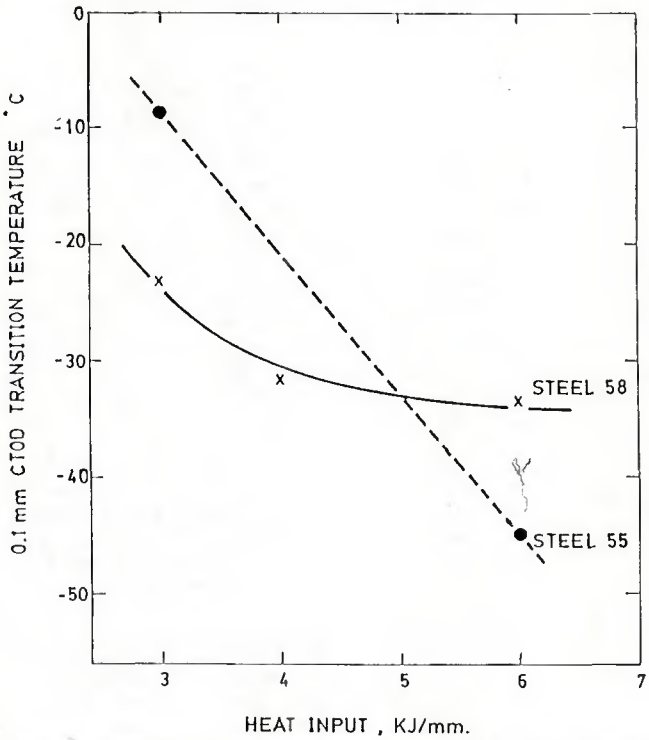

Fig. 4 – 0.1 mm CTOD transition temperature/heat input relations for Steel 55 (Si, Ti) and Steel 58 (V).

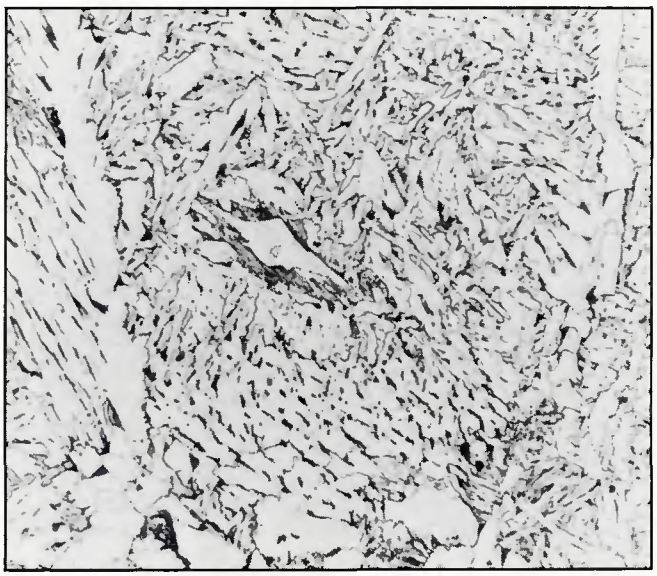

Fig. 5 – HAZ microstructures in Steel 58 (V) at 6 kJ/mm heat input (400X).

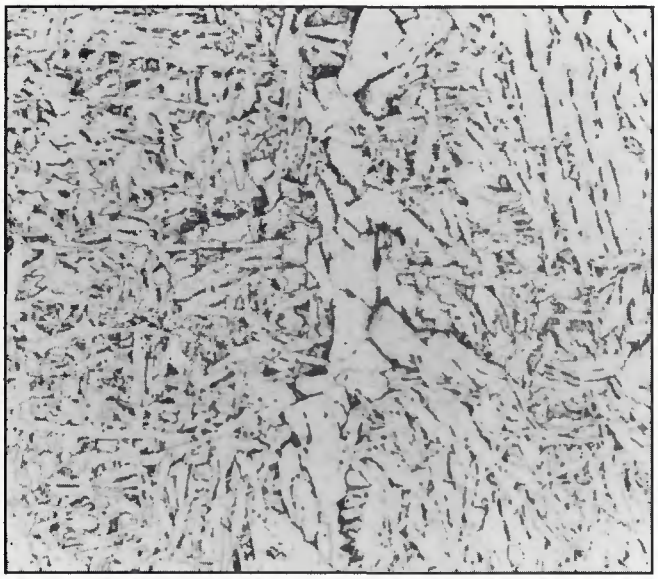

Fig. 6 — HAZ microstructure in Steel 53 (Ti) at 6 kJ/mm heat input (400X).

Fig. 7 — HAZ microstructure in Steel 50 (Nb, V, Ti) 6 kJ/mm (400X).

Table 7 compares the microstructural features in Steels 53, 55 and 56. There was no influence of increasing silicon or decreasing carbon content on the content of the grain boundary ferrite, sideplate ferrite or intragranular phases. Because there is no universal agreement on the terminology for the HAZ microstructural features, Figs. 12 and 13 show the typical microstructures in Steels 55 and 56 for comparison purposes.

Discussion

Banks (Ref. 8) indicated that an initiation criterion of a minimum CTOD of 0.1 mm (0.004 in.) would be sufficient to avoid fracture initiation in welded structures fabricated from steels having yield points up to 350 MPa (50 ksi). Bearing this in mind, minimum CTOD values were plotted at each temperature value, and Figs. 2 to 4 compare the effects of different combinations of microalloying elements on the 0.1 mm CTOD transition temperature values for each steel examined.

The highest HAZ toughness properties at all heat input levels were exhibited by Steel 53, which was microalloyed with titanium only. The poorest HAZ toughness values were in Steel 50, which was microalloyed with niobium, vanadium and titanium. Steel 50 had the highest HAZ hardness (Table 4) and finest grain size of

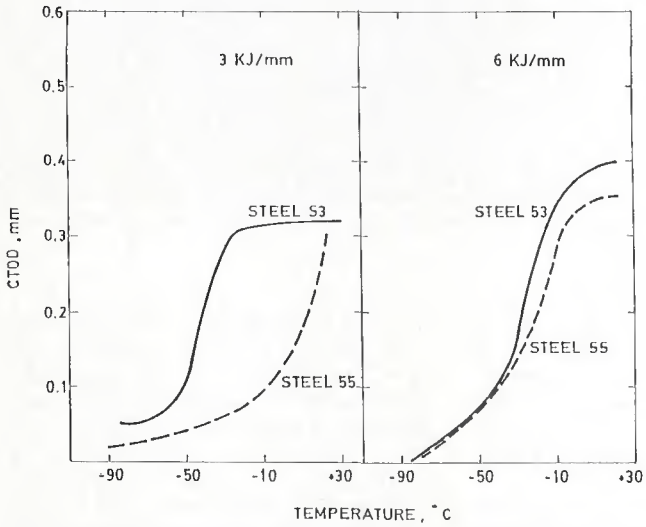

Fig. 8 — CTOD fracture toughness properties of Steel 53 (Ti) and Steel 55 (Si, Ti).

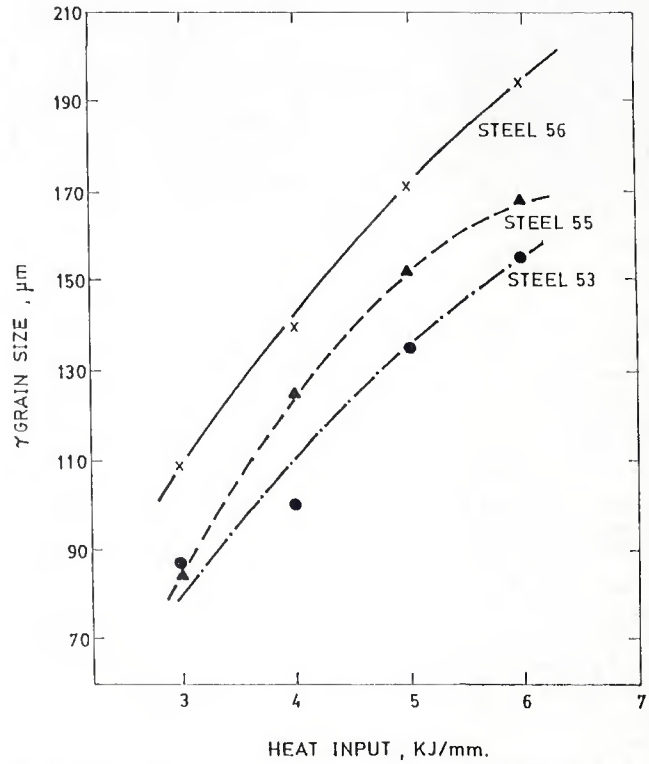

Fig. 9 — HAZ grain size in Steels 53 (Ti), 55 (Si, Ti) and 56 (C, Ti).

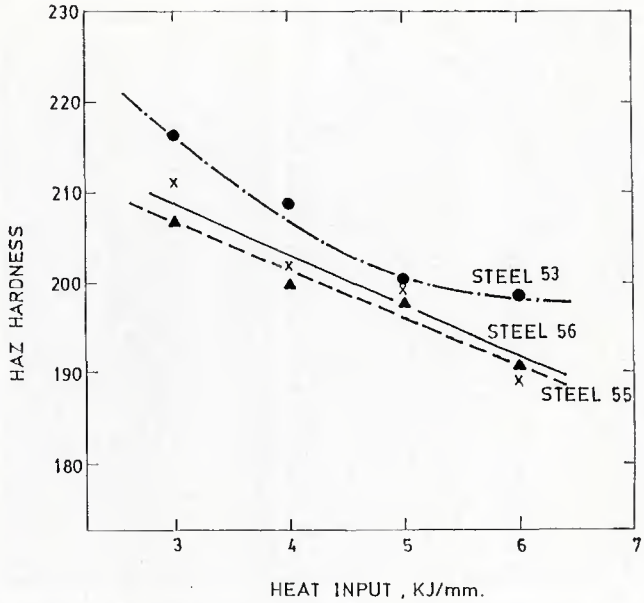

Fig. 10—HAZ hardness in Steels 53 (Ti), 55 (Si, C) and 56 (C, Ti).

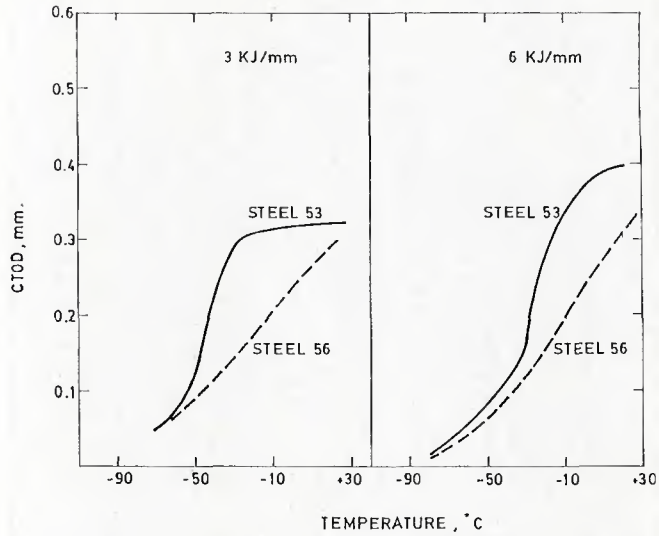

Fig. 11—CTOD fracture toughness properties of Steel 53 (Ti) and Steel 56 (C, Ti).

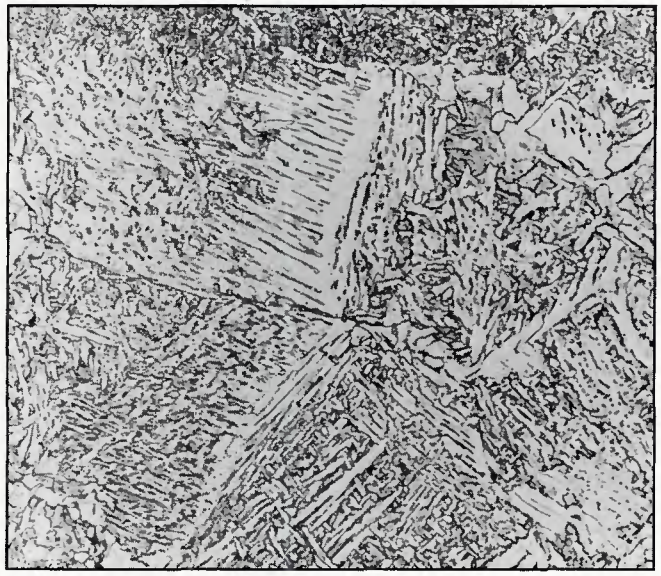

Fig. 12—HAZ microstructure in Steel 55 (Si, Ti) at 3 kJ/mm heat input (400X).

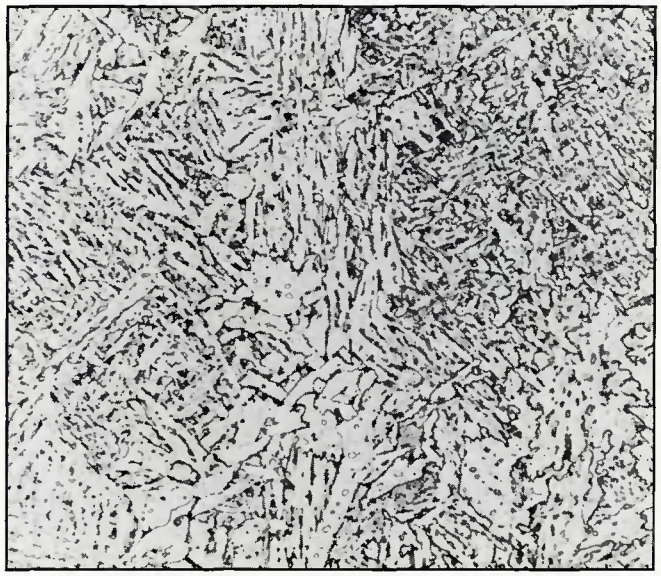

Fig. 13—HAZ microstructure in Steel 56 (C, Ti) at 3 kJ/mm heat input (400X).

all the steels tested. It is clear from Table 5 that Steel 50 (Nb, V, Ti) was significantly stronger than Steel 53 (Ti), and that the employment of combinations of microalloying elements to increase strength properties severely impaired HAZ toughness.

An addition of 0.093% vanadium as a means of increasing plate strength (Steel 58) produced a material that had excellent HAZ fracture toughness properties when it was welded at 6 kJ/mm heat input. However, when welded at 3 kJ/mm the HAZ fracture toughness properties were much poorer since higher hardness values outweighed the beneficial effect of the acicular ferrite-like microstructure—Figs. 4 and 5.

Increasing heat input was particularly detrimental in the case of Steel 51 (V, Ti) and Steel 50 (Nb, V, Ti). In Steel 51 (V, Ti) the 0.1 mm CTOD fracture toughness transition temperature was −46°C when welding at 3 kJ/mm heat input. McCutcheon (Ref. 5) also noted excellent HAZ toughness values in a 0.098%V-0.011%Ti steel welded at a heat input of 2 kJ/mm (51 kJ/in.). However, the 0.1 mm CTOD fracture toughness transition temperature increased 60°C when the heat input was increased from 3 to 6 kJ/mm. Due to this heat input change, the tough acicular ferrite-like structure (in the intragranular constituent) was replaced by a less tough matrix comprising coarse equiaxed ferrite—Table 7.

The detrimental effect of higher heat input on the toughness of steel containing niobium (Steel 59 in Fig. 2) has been well documented (Refs. 4, 9, 10). Both Dolby (Ref. 9) and Hannerz (Ref. 10) ascribed the detrimental niobium effect to higher hardness levels in niobium-bearing steel. In our results, there was no increase in hardness in high heat input welds, and niobium suppressed ferrite formation and promoted formation of intragranular bainite—Table 7.

Yamamato (Ref. 6) has suggested that the detrimental effect of niobium on HAZ toughness properties depends on its microsegregation around TiN precipitates (enhancing hardenability and preventing acicular ferrite nucleation). This suggestion was examined by comparing the perfor-

mance of Steel 53 (Ti) with Steel 52 (Nb, Ti).

In Steel 52 (Nb, Ti), the base metal contained a dispersion of niobium and titanium-rich precipitates prior to welding. A high reheat temperature of 1100°C (2012°F) or above (1150°C was employed for the steels in this study) leads to formation of a coarse distribution of large cuboidal titanium-rich particles, and a fine dispersion of niobium-rich particles prior to welding (Ref. 11). On the heating leg of the weld thermal cycle, the Nb-rich particles dissolve, and if the cuboidal Ti-rich particles are large enough, they will survive the heating cycle. The reheating temperature of the base metal is of critical importance since use of a low reheat temperature of 950°C (1742°F) promotes formation of Nb-rich particles having a narrow composition range and particle size distribution (Ref. 12). When this steel is welded, the heating cycle dissolves the Nb-rich particles and causes precipitation of TiN particles at 1350°C (2462°F). On the cooling leg (for steel with a reheat temperature of 1150°C) niobium precipitates as Nb-rich particles or by forming caps on the surface of Ti-rich particles (Ref. 13). It follows that Yamamato's assertion of Nb microsegregation onto TiN particles markedly depends on the reheat temperature used during production of the base metal.

Comparison of Steel 53 (Ti) with Steel 52 (Nb, Ti) indicated that:

1) the sideplate ferrite content was much higher in Steel 52 (Nb, Ti), see Fig. 14 and Table 7,

2) there was a lower content of intragranular constituents, and consequently, less acicular ferrite, and

3) the 0.1 mm CTOD transition temperatures of Steels 52 (Nb, Ti) and 53 (Ti) were widely different (+2°C *cf* −50°C at 3 kJ/mm heat input in Figs. 2 and 3).

Yamamato (Ref. 6) has indicated that the point of fracture initiation occurs when sideplate ferrite cracks. Consequently, any factor that restricts sideplate ferrite formation (such as acicular ferrite formation) will improve HAZ toughness values. The much higher sideplate ferrite content of Steel 52 (Nb, Ti) *cf* Steel 53 (Ti) could easily explain the wide difference in HAZ toughness values exhibited by these steels. However, this emphasis on sideplate ferrite content rather than acicular ferrite (and its role as the tough microstructural constituent) is not generally supported by our results on Steels 50, 51, 53, 58 and 59. No relation between the 0.1 mm CTOD transition temperature and grain boundary ferrite content, sideplate ferrite content or a combination of these constituents was apparent, and the highest toughness values were associated with HAZ microstructures containing acicular ferrite. In this connection, Luo and Embury (Ref. 14) have also indicated that coarse ferrite in the HAZ microstructure acts as a nucleus for cleavage fracture, and that higher contents of coarse ferrite lower the cleavage fracture stress. In their work, the coarse ferrite content was evaluated by point counting and summating the contents of grain boundary ferrite, ferrite sideplates and intragranular polygonal ferrite. Since yield stress decreased more rapidly than cleavage fracture stress (as coarse ferrite content increased), the transition temperature was lower at high coarse ferrite contents. This explained the lower transition temperatures they observed in the welds deposited at 10 kJ/mm *cf* 2 kJ/mm.

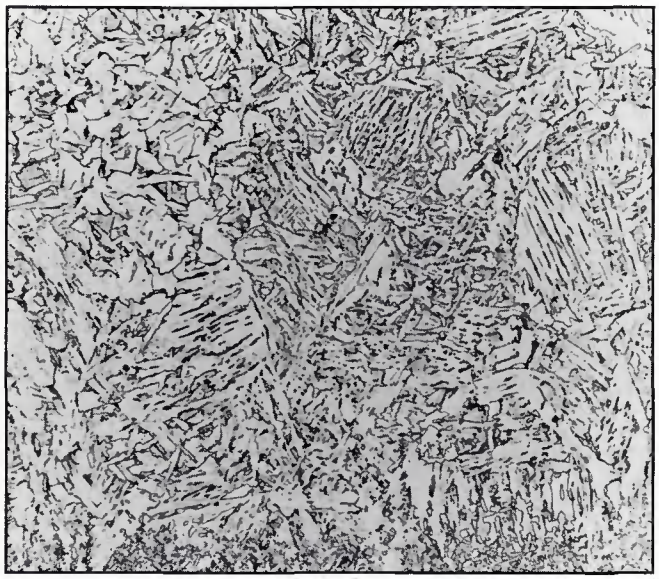

Fig. 14 — HAZ microstructure in Steel 52 (Nb, Ti) at 3 kJ/mm heat input (400X).

It is apparent that the interplay between HAZ microstructure and toughness properties is extremely complex and that the fracture process depends on the combined effects of both coarse ferrite and acicular ferrite constituents.

As indicated previously, the highest fracture toughness values were found in Steel 53 (Ti). Increasing silicon from 0.26 to 0.56% in this type of steel (Steel 55) had an extremely detrimental effect on HAZ toughness properties when welding at 3 kJ/mm — Fig. 8.

Although the prior austenite grain size in Steel 55 was slightly larger (Fig. 9), the HAZ hardness was less — Fig. 10. It is apparent from Table 7 that the intragranular components in Steel 53 (Ti) comprised 20% bainite, and a mixture of acicular ferrite and pearlite. When the silicon content was raised from 0.26 to 0.56% in Steel 55, the increased hardenability contribution prevented formation of the tough acicular ferrite/pearlite structure, and this accounted for the poor fracture toughness properties. The detrimental influence of higher silicon content disappeared at high heat input (6 kJ/mm). In this case, the intragranular component in the HAZ microstructure comprised a mixture of large ferrite laths and smaller ferrite grains — Table 7.

Decreasing the carbon content from 0.11 to 0.077% (in Steel 56) also impaired HAZ fracture toughness properties at 3 and 6 kJ/mm. In particular, the fracture toughness at temperatures above −30°C were significantly decreased — Fig. 11. It is possible that this was due to the difference in intragranular constituents present in Steels 53 (Ti) and 56 (C, Ti), *i.e.*, a mixture of bainite, acicular ferrite and pearlite in Steel 53 (Ti), and irregularly shaped ferrite plates embedded with second phase (carbide/(M-A)phase) particles in Steel 56 (C, Ti).

Conclusions

A detailed evaluation of 0.1 mm CTOD fracture toughness transition temperature values indicated that:

1) HSLA steel microalloyed with a combination of elements (Nb, V, Ti) had much poorer toughness properties than steel alloyed with titanium alone. Increasing silicon content in steel alloyed with titanium only had a detrimental effect on fracture toughness properties in welds made at a heat input of 3 kJ/mm. At 6 kJ/mm heat input, this detrimental influence of higher silicon content was not apparent. In the case of lower carbon content in steel alloyed with titanium only, the fracture toughness values were marginally poorer when welding at high heat input (6 kJ/mm).

2) Increasing heat input from 3 to 6 kJ/mm had a particularly detrimental influence on the HAZ toughness of HSLA steel microalloyed with vanadium and titanium. In this case, the tough acicular ferrite microstructure was replaced by less tough, coarse equiaxed ferrite.

3) HSLA steel containing 0.093% V had excellent HAZ toughness values when

welded at 6 kJ/mm. However, when welding at 3 kJ/mm heat input, HAZ toughness properties were impaired since higher hardness values outweighed the beneficial influence of acicular ferrite in the HAZ microstructure.

4) The combination of titanium plus niobium produced much poorer toughness properties than titanium alone. This effect was due to increased sideplate ferrite and lower acicular ferrite contents in the HAZ microstructure.

References

1. Hvrivnak, I. 1974. HAZ properties in structural steels. *Zvanacski Spravy* (1):3.
2. Dolby, R. E. 1972. Fracture toughness comparison of weld HAZ and thermally simulated microstructures. *Metal Construction* 4(2):59.
3. Suzuki, S., and Weatherly, G. C. 1985. Characteristics of precipitates and grain growth in simulated thermal cycles of Ti-Nb bearing steel weldments. ASM International Conference. Beijing, China.
4. Graville, B., and Rothwell, A. B. Effect of niobium on HAZ toughness using the instrumented Charpy test. *Metal Construction* 9(1):455.
5. McCutcheon, D. B., McGrath, J. T., Godden, M. J., Ruddle, G. E., and Embury, J. D. 1982. Optimization of processing properties and service performance. ASTM-STP-792, Conference Micon-82, Houston, Tex.
6. Yamamato, K., Matsuda, S., Toshiaki, H., Chijiiwa, R., and Mimura, H. 1987. (unpublished research) Nippon Steel Corp., Tokyo, Japan.
7. Lau, T., Wang, G. R., and North, T. H. 1974. HAZ fracture toughness of Ti-containing steels. To be published in *Materials Science and Technology*, The Institute of Metals, U. K.
8. Banks, E. 1974. Toughness properties of HAZ structures in structural steel. *Welding Journal* 56(7):299-s.
9. Dolby, R. E. 1979. HAZ toughness of structural and pressure vessel steels: improvement and predictions. *Welding Journal* 58(8): 22-s.
10. Hannerz, N. 1975. Effect of Nb on the HAZ ductility of construction H. T. steels. *Welding Journal* 54(5):162.
11. Weatherly, G. C. 1988. Precipitation and grain boundary growth phenomena associated with high heat input welding of microalloyed steels. THERMEC Conference, Tokyo, Japan.
12. Suzuki, S., Weatherly, G. C., and Houghton, D. C. 1987. The response of carbonitride particles in HSLA steels to weld thermal cycles. *Acta Metallurgica* 35(2):341.
13. Houghton, D. C., Weatherly, G. C., and Embury, J. D. 1981. Thermomechanical processing of microalloyed austenite. The Metallurgical Society, AIME, p. 267.
14. Luo, L. G., and Embury, J. D. 1987. The relationship between COD transition temperature and HAZ structures in HSLA steel. Dept. of Materials Science and Engineering, McMaster University, Hamilton, Ont., Canada. Internal report.

WRC Bulletin 339
December 1988

Development of Tightness Test Procedures for Gaskets in Elevated Temperature Service
By A. Bazergui and L. Marchand

In this report, different elevated temperature gasket tightness test procedures are compared. A two-tier test approach, involving aging of the preloaded gasket in a kiln followed by a short duration tightness test was evaluated. The procedures were evaluated using spiral-wound gaskets with two different fillers: a mica-graphite filler and an asbestos filler.

Publication of this report was sponsored by the Subcommittee on Bolted Flanged Connections of the Pressure Vessel Research Committee of the Welding Research Council. The price of WRC Bulletin 339 is $16.00 per copy, plus $5.00 for postage and handling. Orders should be sent with payment to the Welding Research Council, 345 E. 47th St., Suite 1301, New York, NY 10017.

WRC Bulletin 343
May 1989

Destructive Examination of PVRC Weld Specimens 202, 203 and 251J

This Bulletin contains three reports:

(1) Destructive Examination of PVRC Specimen 202 Weld Flaws by JPVRC
By Y. Saiga

(2) Destructive Examination of PVRC Nozzle Weld Specimen 203 Weld Flaws by JPVRC
By Y. Saiga

(3) Destructive Examination of PVRC Specimen 251J Weld Flaws
By S. Yukawa

The sectioning and examination of Specimens 202 and 203 were sponsored by the Nondestructive Examination Committee of the Japan Pressure Vessel Research Council. The destructive examination of Specimen 251J was performed at the General Electric Company in Schenectady, N.Y., under the sponsorship of the Subcommittee on Nondestructive Examination of Pressure Components of the Pressure Vessel Research Committee of the Welding Research Council. The price of WRC Bulletin 343 is $24.00 per copy, plus $5.00 for U.S., or $8.00 for overseas, postage and handling. Orders should be sent with payment to the Welding Research Council, Room 1301, 345 E. 47th St., New York, NY 10017.